LBL-16574
CONF-8310121--6

Lawrence Berkeley Laboratory
UNIVERSITY OF CALIFORNIA

EARTH SCIENCES DIVISION

Presented at the 58th Annual Society of Petroleum Engineers of AIME Technical Conference and Exhibition, San Francisco, CA, October 5-8, 1983

PRESSURE TRANSIENT METHOD FOR FRONT TRACKING

S.M. Benson and G.S. Bodvarsson

August 1983

LBL--16574

DE84 002913

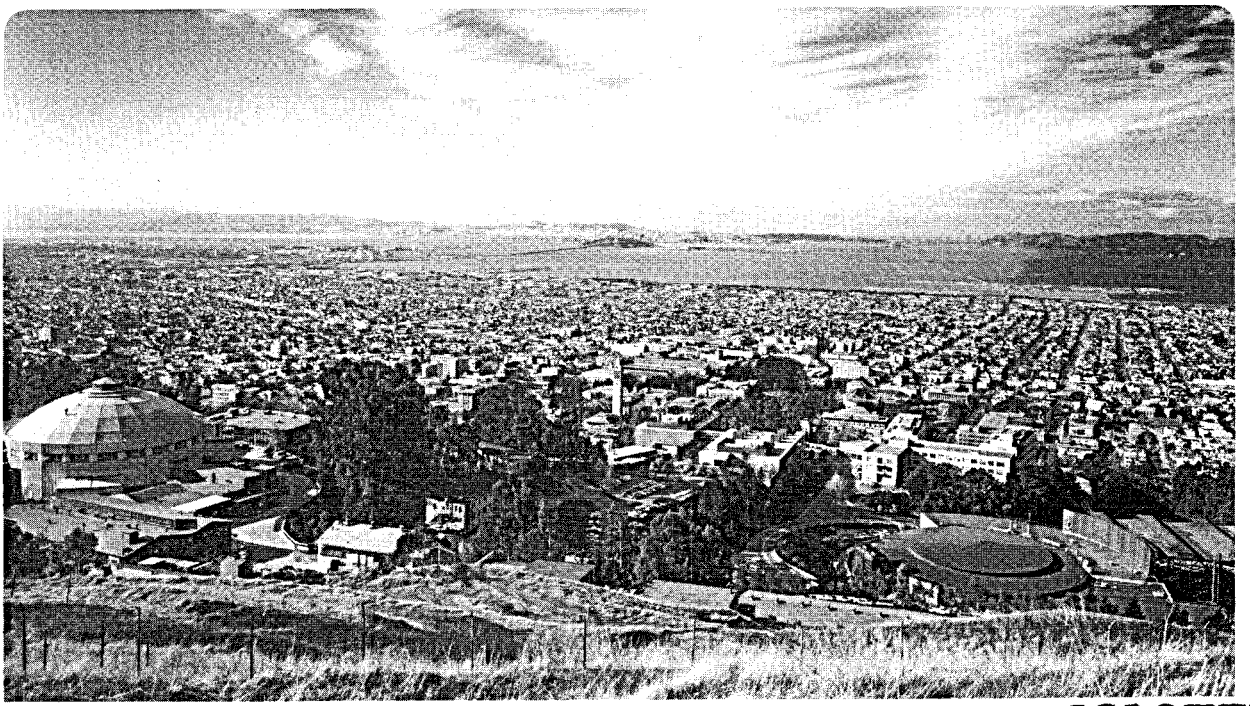

Prepared for the U.S. Department of Energy under Contract DE-AC03-76SF00098

DISCLAIMER

To be presented at the 58th Annual Society of Petroleum Engineers of AIME Technical Conference and Exhibition, San Francisco, CA, October 5-8, 1983

LBL-16574

PRESSURE TRANSIENT METHOD FOR FRONT TRACKING

S.M. Benson and G.S. Bodvarsson

Earth Sciences Division
Lawrence Berkeley Laboratory
University of California
Berkeley, California 94720

ABSTRACT

A pressure transient technique for tracking the advance of cold water fronts during water flooding and geothermal injection operations has been developed. The technique is based on the concept that the steady state pressure buildup in the reservoir region inside the front can be calculated by a fluid skin factor. By analyzing successive pressure falloff tests, the advance of the front in the reservoir can be monitored. The validity of the method is demonstrated by application to three numerically simulated data sets, a nonisothermal step-rate injection test, a series of pressure falloffs in a multilayered reservoir, and a series of pressure falloff tests in a water flooded oil reservoir.

INTRODUCTION

During both geothermal and water flooding operations it is important to know the position of the interface or front between the injected and in situ fluids. Since the injected fluid usually has a different viscosity, density and relative permeability than that of the in situ fluid, injection creates a radially symmetric heterogeneity around the well.

Pressure transients during injection and falloff, in systems with radial discontinuities created by fluid injection, have been studied by numerous researchers[1-12]. These studies have shown that under a variety of specific conditions, the reservoir properties and the skin factor can be determined from injection test or falloff data. Benson and Bodvarsson[13] showed that the region around the well created by cold water injection into a hot reservoir could be mathematically treated by a thermal skin factor. Benson[14] extended this concept to develop a method of front tracking during cold water injection into a hot water reservoir. A generalized formulation of the fluid skin factor and how it can be used for front tracking is developed in this paper.

References and illustrations at end of paper.

BACKGROUND

Pressure transients during injection of fluids with different properties are characterized by one of two types of behavior:

(1) Moving front-dominated behavior, during which the very early time pressure transients correspond to the properties of the reservoir fluid and the late time transients to the properties of the injected fluid[9,10,13]

(2) Composite reservoir (stationary front) behavior which is characterized by two slopes, the first corresponding to the fluid properties of the region inside the front and the second to the properties of the reservoir fluid outside of the front.[13]

This study applies to pressure transients characterized by the composite-reservoir behavior.

The thermal skin factor, which can be generalized to a fluid skin factor, is best explained by considering the pressure buildup and falloff due to nonisothermal injection. Figure 1 shows numerically simulated pressure buildup data for a step rate test during which 20°C water is injected into a 250°C reservoir (a mobility contrast of nearly 10). For comparison, isothermal injection at 20°C and 250°C, for identical step rate tests, are also shown. Note that the magnitude of the pressure buildup for the nonisothermal test is less than that for 20°C isothermal injection and greater than that for isothermal 250°C injection. In other words, relative to the hot reservoir, the cold water creates an additional buildup component that depends on the mobility contrast between the two fluids. The thermal skin factor is derived in the same way as the mechanical skin factor and can be expressed as

$$s_t = \left(\frac{\mu_i}{\mu_o}\,\frac{\rho_o}{\rho_i} - 1\right)\ln\frac{r_f}{r_w} \qquad (1)$$

The present study discusses a method of front tracking which requires successive pressure falloff tests, or step rate injection tests be conducted.

The method is based on the relationship between the increasing radial distance to the injection front and the resultant changes in the fluid skin factor (defined below).

APPROACH

An expression for the fluid skin factor can be derived analytically by considering the steady state pressure response in a two-fluid composite reservoir. In this paper, the fluid skin factor is derived and then its use as a method of front tracking is developed. The applicability and validity of the method is demonstrated by analyzing numerically simulated pressure falloff data in both nonisothermal liquid water and oil-water systems. Two computer programs are used, PT and STMFLD. Both use the integral finite-difference method for discretizing the medium and formulating the governing equations.[16]

PT solves both the mass and energy balance equations in a water-saturated porous and/or fractured medium. The fluid viscosity, density, compressibility, and thermal expansivity are all calculated internally as functions of temperature and pressure to within 1% of their correct value. The code has been validated against many analytic solutions and field data. A detailed description of PT is given by Bodvarsson[17].

STMFLD is a multidimensional, fully-implicit numerical model for simulating steam and water flooding of hydrocarbon reservoirs[18]. The model formulation includes two hydrocarbon components, thus, three mass- and one energy-balance equations are solved for each grid block. Both PT and STMFLD use an efficient, direct solution technique[19].

THEORY

The present study is applicable to a reservoir/well system which is shown schematically in Figure 2. We assume that the reservoir is:

(1) uniform and has a constant porosity, permeability, heat capacity, and thermal conductivity;

(2) horizontal, infinite, and bounded above and below by impermeable and insulating strata;

(3) fully saturated with one or more liquids;

(4) fully penetrated with a finite radius well bore.

The near-well region may have a different permeability than the reservoir but it must remain unaltered throughout injection.

The effects of gravity are neglected in the study. In later sections the possibility of applying this method to a layered or fractured reservoir is discussed.

The front tracking methods discussed here are applicable to reservoirs described above when the pressure transients behave like those of a composite reservoir system. A detailed discussion of when the pressure transients for nonisothermal injection behave like those of a composite system is given by Benson and Bodvarsson[13]. Pressure falloffs always behave according to the composite system model (stationary front) therefore, the emphasis of this paper is on the analysis of pressure falloff tests.

The steady-state pressure buildup in a two-fluid composite system with a stationary front is given by

$$\Delta P = \frac{Q_o \mu_o}{2\pi k k_{ro} H}\left[\left(\frac{k_{ro}\mu_i\rho_o}{k_{ri}\mu_o\rho_i}\right)\ln\frac{r_f}{r_w} + \ln\frac{r_e}{r_f}\right] \quad (2)$$

By rearranging and adding and substracting the term $\ln r_f/r_w$, equation (2) can be written

$$\Delta P = \frac{Q_o \mu_o}{2\pi k k_{ro} H}\left[\left(\frac{k_{ro}\mu_i\rho_o}{k_{ri}\mu_o\rho_i} - 1\right)\ln\frac{r_f}{r_w} + \ln\frac{r_e}{r_w}\right] \quad (3)$$

By analogy to the mechanical skin factor, the fluid skin factor can be defined

$$s_f = \left(\frac{k_{ro}\mu_i\rho_o}{k_{ri}\mu_o\rho_i} - 1\right)\ln\frac{r_f}{r_w} \quad (4)$$

If there is a region of mechanical damage or enhancement around the wellbore, the steady-state pressure buildup has three components, one due to the mechanical skin, another due to the flooded region, and a third one due to the reservoir. Assuming that the near-well region has been flooded, the steady-state pressure drop can be expressed as

$$\Delta P = \frac{Q_o \mu_o}{2\pi k k_{ro} H}\left[\left(\frac{k_{ro} k \mu_i\rho_o}{k_{ri} k_s \mu_o\rho_i} - 1\right)\ln\frac{r_s}{r_w} + \left(\frac{k_{ro}\mu_i\rho_o}{k_{ri}\mu_o\rho_i} - 1\right)\ln\frac{r_f}{r_s} + \ln\frac{r_e}{r_f}\right] \quad (5)$$

For most practical cases, the term $\ln r_f/r_s$ can be approximated by r_f/r_w and once again, the concept of a fluid skin factor can be used. It is also of interest to note that the total apparent skin factor has two components, that is

$$s_a = \left(\frac{k_{ro} k \mu_i\rho_o}{k_{ri} k_s \mu_o\rho_i} - 1\right)\ln\frac{r_s}{r_w} + s_f \quad (6)$$

In this expression the true mechanical skin of the well is combined with fluid-related components.

In order to use the fluid skin factor as a front tracking tool, a test and analysis procedure must be developed that will allow differentiation between the mechanical and fluid skin factors of a well. In cases where the front between the injected and reservoir fluid moves as a function of t/r^2, which is the case for most processes considered in porous medium, such a procedure

can be developed as follows. The radial position of the front can be expressed as

$$r_f = \left(\frac{aQt}{\pi H}\right)^{1/2} \tag{7}$$

where a is a constant of proportionality that depends on the mass-and energy-balance equations governing the displacement process. For example,

$$a = \frac{\rho_w c_w}{\rho_a c_a} \tag{8a}$$

and

$$a = \frac{1}{\phi}\left.\frac{df_w}{ds_w}\right|_{s_{wf}} \tag{8b}$$

for nonisothermal injection and waterflood displacement respectively.[20,21] Noting that the term Qt can be replaced by the cumulative injection C and substituting this expression into Equation (4), we see that

$$s_f = 1.151\left(\frac{\mu_i\rho_o k_{ro}}{\mu_o\rho_i k_{ri}} - 1\right)\left[\log C + \log\frac{a}{\pi H r_w^2}\right] \tag{9}$$

Since the second logarithmic term is a constant, it is clear that a plot of the logarithm of the cumulative injection versus the fluid skin factor will result in a semilog straight line with a slope of

$$n = 1.151\left(\frac{\mu_i\rho_o k_{ro}}{\mu_o\rho_i k_{ri}} - 1\right) \tag{10}$$

Until more than a single wellbore volume has been injected into the formation ($C = \pi r_w^2 H$) the fluid skin factor is zero. Therefore, if successive pressure falloff tests are conducted, after increasingly larger quantities of cumulative injection, the calculated apparent skin values, when plotted versus the logarithm of the cumulative injection, will result in a straight line of slope n. The intercept, evaluated when the fluid skin factor equals zero ($C = \pi r_w^2 H$) will yield the apparent mechanical skin factor.

$$s_{ma} = \left(\frac{k_{ro}k\mu_i\rho_o}{k_{ri}k_s\mu_o\rho_i} - 1\right)\ln\frac{r_s}{r_w} \tag{11}$$

The fluid skin factor can then be evaluated from

$$s_f = s_a - s_{ma} \tag{12}$$

From the fluid skin factor, the radial distance to the front can be calculated

$$r_f = r_w e^{(1.151\, s_f/n)} \tag{13}$$

In Table 1, the radial distance to the front is given as a function of $1.151 s_f/n$. For small values of this term, there is good resolution of the radial distance to the front. However, at large values of $1.151\, s_f/n$, small errors in the calculated fluid skin factor result in large errors in the computed radial distance to the front. Therefore, the front tracking method discussed in this paper is most useful for front tracking during the early phases of injection.

EXAMPLES

Examples are given which demonstrate the application of this method to three different situations, (1) a step rate injection test when 20°C water is injected into a 250°C reservoir, (2) three successive pressure falloff tests in a multilayer reservoir,and (3) two successive pressure falloff tests in a water-flooded reservoir.

Step Rate Injection Test

The following simulation was run to demonstrate front tracking during a step rate injection test. Three six-hour steps, with injection rates of .1 kg/s, .2 kg/s, and .3 kg/s were followed by a complete shutin. The simulated pressure data are shown in Figure 1. Table 2 lists the reservoir and fluid properties used in the simulation. The pressure data from step 1 are not suitable for the type of analysis proposed in this paper because the moving thermal front dominates the pressure transients[13]. Data from steps 2, 3, and 4 (falloff) are suitable for this analysis. A semilogarithmic plot of the data from the pressure falloff are shown in Figure 3. Conventional multirate theory is used in the analysis. For comparison, data from identical step tests in isothermal 20°C and 250°C reservoirs are also shown.

The time at which shutin occurs coincides with the left axis of the graph. At very early times after shutin the data follow a slope which corresponds to the properties of the injected 20°C fluid. At approximately 35 seconds the data begin to depart from the first slope and after several minutes become identical to the falloff in the isothermal 250°C reservoir. This two-slope behavior is typical of two-fluid composite reservoirs. The time at which the pressure transients depart from the first slope can be estimated from the radius of investigation

$$t = \frac{r_f^2\phi\mu_i\beta_t}{4kk_{ri}} \tag{14}$$

For relatively small cold spots (up to 10 m) the first slope is usually masked by wellbore storage, hence the observed semilog straight line will correspond to fluid properties of the reservoir. It is this second slope which must be used to calculate the reservoir permeability and apparent skin factor. From this slope (M_o) and its extrapolation to obtain P_{1s}, the reservoir permeability and the apparent skin factor are calculated:

$$k = \frac{.183Q_o\mu_o}{m_o k_{ro} H} \tag{15}$$

$$s_a = 1.151\left(\frac{P_{wf} - P_{1s}}{m_o} - \log\frac{kk_{ro}}{\phi\mu\beta_t r_w^2} - .351\right) \tag{16}$$

or in the case of a step rate test

$$k = .183 \frac{Q_{o_n} \mu_o}{m_o k_{ro} H} \quad (17)$$

and

$$s_a = 1.151 \left[\frac{Q_{o_n}}{\left(Q_{o_n} - Q_{o_{n-1}}\right)} \frac{\left(P_{wf} - P_{1s}\right)}{m_o} - \log \frac{kk_{ro}}{\phi \mu \beta_t r_w^2} - .351 \right] \quad (18)$$

Just prior to the pressure falloff, the front has advanced 1.6 m into the formation. The calculated permeability is 10^{-14} m^2 and the apparent skin factor, 19.8. A similar analysis of steps 2 and 3 yielded the same transmissivity and apparent skin values of 14 and 18.9, respectively. These apparent skin values versus the logarithm of the cumulative injection are shown in the lowest curve of Figure 4. As expected, they fall on a straight line with a slope of 7.95, which is in good agreement with the value calculated by Equation (10), 8.05. The radial distances to the front were calculated for each step using Equation (13). The calculated values of .65 m, 1.2 m and 1.5 m agree well with the observed values of .7 m, 1.3 m and 1.6 m.

Identical step tests were run for wells with mechanical skin factors of 2 and 5. The calculated apparent skin factors are also shown in Figure 4 and display similar behavior to that of the well with a skin factor of zero, except the intercepts at a cumulative injection of $\pi r_w^2 H$ are displaced. For both of these cases, the fluid factor must be calculated from Equation (12). The remainder of the analysis is identical to that for a well with a mechanical skin factor of zero.

It is important to note that if the mechanical skin factor of a well changes in response to injection, the slope of the line on the s_a versus C curve will not be equal to that given by Equation (10). Similarly, if the movement of the front cannot be expressed as a simple function of t/r^2, the slope will also differ from that predicted by that equation.

Layered Reservoir

In order to determine the applicability of the proposed front tracking method to a layered reservoir, the pressure falloff following injection of 50°C water into a 250°C three-layer reservoir was simulated. The reservoir and fluid properties used are listed in Table 2. A schematic of the reservoir is shown in Figure 5.

Pressure falloffs were simulated after three different periods of injection at a rate of 30 kg/s; 10^4 s, 2.5×10^4 s and 10^5 s. Horner graphs of each falloff are shown in Figure 6. Note that by nondimensionalizing the data using $(t + \Delta t)/\Delta t$ causes all of the data to fall on one curve. All the data display typical two-fluid composite-reservoir behavior. Also note that the values of P_{1s} are shown on the graph for each of the falloff tests.

The data can be analyzed to obtain the average permeability ($\bar{k}$) from the slope corresponding to the reservoir fluid properties. The calculated value of $\bar{k}$, 6.7×10^{-14} m^2, is very close to the correct value of 6.66×10^{-14} m^2. The apparent skin can also be calculated using Equation (16), if $\bar{k}$ is substituted for k. The calculated values of the apparent skin are 9.73, 11.23 and 13.44. A plot of the apparent skin values is shown in Figure 7. Once again, the data fall on a straight line. The slope of the line is 3.71, which is close to the value of 3.61 computed using Equation (10). The line extrapolates to a value of zero when the cumulative injection equals $\pi r_w^2 H$. This is consistent with the zero skin value used in the simulation.

In Figure 8, the radial distance to the thermal front is shown in each of the three layers. Note that the front has extended farthest from the well in the most permeable layer. The radial distance to the front after each period of injection can be calculated from Equation (13). The respective values are 2.2 m, 3.5 m, and 7.1 m. Comparison between these values and those shown in Figure 7 indicates that the values predicted from Equation (13) are midway between the distance to the front in the more permeable stratum and the distance to the front in the less permeable strata. This cannot be considered a rigorous analysis of front penetration in layered formations. It does, however, indicate that the small-scale heterogeneity prevalent in most formations will not significantly reduce the effectiveness of this method for front tracking.

Water Flood Falloff

There are two major differences, important to pressure transient analysis, between cold water injection into a hot-water reservoir and cold water injection into an oil reservoir. First, in general, the water has a higher mobility that the in situ oil, thus the fluid skin factor has a negative rather than a positive value. Second, water flooding usually results in a diffuse region behind the front where the water saturation varies from $s_w = 1 - s_{or}$ immediately adjacent to the well to another value at the front, which is governed by the relative mobilities and capillary pressure. In comparison, cold water injected into a hot reservoir results in a nearly uniform temperature around the well with a relatively small transition zone that separates the cold and hot regions.

A numerical simulation of the pressure falloff after isothermal water flooding of an oil reservoir demonstrates the applicability of the front tracking method discussed in this paper. The reservoir and fluid properties used are listed in Table 2. The relative permeability of the oil and water phases were calculated from simple X-curves as follows:

$$k_{rw} = k_{ri} = (s_w - .3)/.7 \quad (19a)$$

$$k_{ro} = 1 - s_w/.8 \quad (19b)$$

The irreducible oil and water saturations are .2 and .3, respectively. Using the fluid properties listed in Table 2 and the relative permeability curves given above, a Buckley-Leverett analysis of the flooding process predicts an average water saturation of approximately 0.45 behind the front and .38 at the front[20].

Horner plots of the simulated pressure falloffs after 10^5 s and 10^6 s of water flooding at a rate

of .05 kg/s are shown in Figure 9. As expected, the same two-slope behavior, typical of a composite system, is observed. In this case however, the first slope is smaller than the second, indicative of a more mobile inner region. The slope of the first straight line corresponds to the fluid properties of the water for a relative permeability evaluated at the irreducible oil saturation. This results from the fact that the reservoir rock immediately adjacent to the wellbore is rapidly flooded by many pore volumes of water and consequently the oil saturation rapidly approaches the irreducible oil saturation. Since the region immediately adjacent to the well is so important to the pressure transients observed at the well, it is this fully swept region which controls the early-time transients and governs the steady-state pressure change associated with the fluid skin factor.

The slope on the semilogarithmic straight line of the simulated data can be analyzed to determine the formation permeability. From P_{1s}, k_{ri} evaluated at the irreducible oil saturation and k_{ro} evaluated at the oil saturation in the undisturbed reservoir, the apparent skin values can be calculated by Equation (16). Apparent skin values of -1.77 and -2.78 are calculated for the pressure falloffs following 10^5 s and 10^6 s of injection, respectively. The slope of the line on the apparent skin factor vs. cumulative injection curve is -1.01, which is in good agreement with the value of -1.05 calculated from Equation (10).

The radial distance to the front can be calculated from the apparent skin factor using Equation (13). Radial distances to the front of .9 m and 2.1 m are calculated after injection for 10^5 s and 10^6 s, respectively. The saturation profiles in the reservoir are shown in Figure 10. Note that in each instance, the calculated distance to the front occurs at a water saturation of approximately .55, nearly midway between the irreducible oil saturation and undisturbed reservoir saturation. This example demonstrates that even though the simple composite reservoir model is not strictly applicable to water-flood displacement, the completely swept near-well region dominates the pressure response and therefore allows successful application of the front tracking technique.

FRONT TRACKING IN FRACTURED RESERVOIRS

In the above discussion we have only considered porous medium, single-phase reservoirs. However, most geothermal reservoirs, and many oil reservoirs, are fracture-dominated. Also, there may be the additional complexity of a gas phase flowing in the reservoir. Thus, the extent to which the methodology developed in this paper is applicable to these more complex situations needs to be examined.

Bodvarsson et al.[22] and Bodvarsson and Benson[23] studied nonisothermal injection/falloff tests in reservoirs with horizontal fractures. In their studies fluid flow takes place in the fractures and the rock matrix conducts heat to the fracture fluids. In the case of injection tests, the pressure transient data can be analyzed using the conventional Theis-type methods, providing the average fluid properties (ρ, μ) are used (i.e., the fluid properties should be calculated based on the average temperature, $T_{ave} = 1/2(T_{in} + T_r)$). The reason for this is that in a fracture system, the speed of the cold water front is proportional to r^4/t.[24] The falloff data can be analyzed in the manner discussed above; however in estimating the radial distance to the cold water front one must consider the advancement rate of the cold water front along the fractures given by Bodvarsson and Tsang[24]

$$r_f = \left(\frac{t}{4.396 \lambda \rho_r C_r} \left(\frac{\rho_w c_w Q}{\pi} \right)^2 \right)^{1/4}$$

In the case of a reservoir with an existing cold spot (i.e., after considerable injection) the injection/falloff test data should be analyzed using the fluid properties corresponding to the hot reservoir fluids.[23] Therefore, with some modification, the proposed front tracking method should be applicable to fractured and/or fractured porous mediums.

CONCLUSIONS

A method for tracking fronts during waterflooding or geothermal injection operations has been developed. The method is based on the concept of a fluid skin factor. This front tracking method requires that conventional pressure falloff tests be conducted after increasing periods of injection. Three examples are given which demonstrate application of the method to: 1) step-rate injection tests; 2) falloff tests in layered reservoirs, and 3) falloff tests in waterflooded reservoirs.

The method is most successfully applied early during waterflood or geothermal injection operations when the resolution of the radial distance to the front is greatest. The technique is applicable to many two-fluid composite systems in which the movement of the front depends on t/r^2. It may also be possible, with minor modifications, to extend this method to fractured systems where the front advances at a rate that is proportional to t/r^4.

NOMENCLATURE

- a - constant of proportionality (-)
- c - heat capacity (J/kg.°C)
- C - cumulative injection (m^3)
- f_w - fractional flow of water
- H - reservoir thickness (m)
- k - permeability (m^2)
- k_r - relative permeability (-)
- $\bar{k}$ - average permeability (m^2)
- m - absolute value of the slope on the linear segment of the semilogarythmic plot (Pa/cy)
- P - pressure (Pa)
- P_{wf} - flowing pressure prior to shut-in (Pa)
- P_{1s} - extrapolated pressure at one second after shut-in (Pa)
- q - mass flow rate (kg/s)
- Q - volumetric flow rate (m^3/s)
- Q_{o_n} - volumetric injection rate at step n(m^3/s)
- r_c - radius of the cold spot (m)
- r_e - radial distance to constant pressure boundary (m)
- r_f - radial distance to the front (m)
- r_s - radius of the damaged or enhanced region (m)

r_w - well radius (m)
s - skin factor (-)
s_a - apparent skin factor
s_f - fluid skin factor (-)
s_{ma} - apparent mechanical skin factor
s_{or} - irreducible oil saturation
s_t - thermal skin factor (-)
s_w - water saturation (-)
t - time (s)
T - temperature (°C)

GREEK LETTERS

β_t - total system compressibility (Pa^{-1})
Δ - difference
λ - thermal conductivity (J/s.m.°C)
μ - viscosity (Pa.s)
ρ - density (kg/m^3)
φ - porosity (-)

Susbcripts

a - aquifer
f - front
i - inside the front
in - injection
o - outside the front
r - reservoir
w - water

ACKNOWLEDGEMENTS

Critical review of this manuscript by M.J. Lippmann of Lawrence Berkeley Laboratory is gratefully appreciated.

This work was supported by the Assistant Secretary for Conservation and Renewable Energy, Office of Renewable Technology, Division of Geothermal and Hydropower Technologies of the U.S. Department of Energy under Contract no. DE-AC03-76SF00098.

REFERENCES

1. Hazebroek, P., Rainbow, H., and Matthews, C.S., "Pressure Fall-Off in Water Injection Wells," Trans., AIME (1958) 213, 250-260.

2. Bixel, H.C. and van Poollen, H.K.: "Pressure Drawdown and Buildup in the Presence of Radial Discontinuities," Soc. Pet. Eng. J. (Sept. 1967) 301-309; Trans., AIME, 240. Also Reprint Series, No. 9 -- Pressure Analysis Methods, Society of Petroleum Engineers of AIME, Dallas (1967) 188-196.

3. van Poollen, H.K.: "Transient Tests Find Fire Front in an In-Situ Combustion Project," Oil and Gas J. (Feb. 1, 1965) 78-80.

4. Ramey, H.J., Jr., Kumar, A., and Gulati, M.S.: Gas Well Test Analysis Under Water-Drive Conditions, AGA, Arlington, Va. (1973).

5. Mangold, D.C., Tsang, C.F., Lippmann, M.J.,.and Witherspoon, P.A.: "A Study of Thermal Discontinuity in Well Test Analysis," Journal of Petroleum Technology (June, 1981), v. 33, No. 6.

6. Satman, A., Eggenschwiller, M., Tang, R.W., and Ramey, H.J.: "An Analytical study of Transient Flow in Systems with Radial Discontinuities", SPE 9399, September, 1980.

7. Kazemi, Hossein, Merrill, L S., and Jargon, J.R.: "Problems in Interpretation of Pressure Fall-Off Tests in Reservoirs With and Without Fluid Banks," J. Pet. Tech. (Sept. 1972) 1147-1156.

8. Merrill, L.S., Jr., Kazemi, Hossein, and Gogarty, W. Barney: "Pressure Falloff Analysis in Reservoir With Fluid Banks," J. Pet. Tech. (July 1974) 809-818; Trans., AIME, 257.

9. Bodvarsson, G.S. and Tsang, C.F.: "Thermal Effects in the Analysis of Fractured Reservoirs" in 3rd Invitational Well Testing Symposium, Lawrence Berkeley Laboratory Report, LBL-12076, Berkeley, California, March, 1980.

10. Tsang, Y. W., and C. F. Tsang, An Analytic Study of Geothermal Reservoir Pressure REsponse to Cold Water Reinjection, Proceedings 4th Workshop on Geothermal Reservoir Engineering Stanford University, Stanford, California, SGP-TR-30, 322-331, (December 13-15) 1978.

11. O'Sullivan, M. J., and K. Pruess, "Analysis of Injection Testing of Geothermal Reservoirs," Geothermal Resources Council, 4, (September) 1980.

12. Garg, S. K. Pressure Transient Analysis for Two-phase (Liquid Water/Steam) Geothermal Reservoirs: SPE 7479, presented at the SPE 53rd Annual Meeting, Houston, Texas, (October 1-3) 1978.

13. Benson, S. M. and Bodvarsson, G. S.: "Non-isothermal Effects During Injection and Falloff Tests," SPE paper 11137, presented at the 57th Annual Meeting of the Society of Petroleum Engineers, New Orleans, Louisiana, 1982.

14. Benson, S. M.: "Interpretation of Nonisothermal Step-Rate Injection Tests", in, Proceedings of the 8th Workshop on Geothermal Reservoir Engineering, Stanford, California, 1982.

15. Earlougher, Jr., R. C. Advances in Well Test Analysis, Society of Petroleum Engineers, Monograph 5, 1977.

16. Edwards, A. L., TRUMP: A Computer Program for Transient and Steady state Temperature Distribution in Multidimensional Systems, Lawrence Livermore Laboratory, Livermore, California, UCRL-14754, Rev. 3, 1972.

17. Bodvarsson, G.S., "Mathematical Modeling of the Behavior of Geothermal Systems under Exploitation," Ph.D. dissertation, University of California, Berkeley, 1981.

18. Pruess, K., and G.S. Bodvarsson, "STMFLD User's Manual", report submitted to the Energy Resources Company, Walnut Creek, California, March 1982.

19. Duff, I.S., MA28--A Set of Fortran Subroutines for Sparse Unsymmetric Linear Equations, Report AERE - R 8730, Harwell/Oxfordshire, Great Britain, 1977.

20. Bodvarsson, G., On the Temperature of Water Flowing Through Fractures, Journal of Geophysical Research, 74, 8, (April) 1969.

21. Buckley, S.E. and M.C. Leverett, Mechanism of Fluid Displacement in Sands; Trans. AIME, 146; 1942, p. 107-116.

22. Bodvarsson, G.S., Benson, S.M., Sigurdsson, O., Stefansson, V. and E.T. Eliasson, The Krafla Geothermal Field, Iceland, 1. Analysis of well test data, submitted to the Journal of Water Resources Research, 1983.

23. Bodvarsson, G.S., and S.M. Benson, Analysis of Nonisothermal Injection Tests in Fractured Reservoirs, paper in preparation, 1983.

24. Bodvarsson, G.S. and C.F. Tsang., Injection and Thermal Breakthrough in Fractured Geothermal Reservoirs, J. Geophy. Research, Vol. 87, No. BL, p. 1031-1048, Feb. 1982.

Table 1. Radial distances to the front for several values of $1.151 s_f/n$ (well radius = .1 m).

$1.151 s_f/n$	r_f
.1	0.11 m
.2	0.12 m
.3	0.13 m
.4	0.15 m
.5	0.16 m
1.0	0.27 m
2.0	0.74 m
3.0	2.00 m
4.0	5.46 m
5.0	14.84 m
6.0	40.34 m

Table 2. Reservoir and fluid properties used in the numerical simulations.

Parameter		Step Rate Test	Layered Reservoir	Water Flood
k	(m^2)	10^{-14}	5×10^{-14}, 10^{-13}, 5×10^{-14}	10^{-13}
H	(m)	1	10, 10, 10	10
ϕ	(-)	.2	.2	.2
c_r	(J/kg°C)	1000	1000	1000
ρ_r	(kg/m^3)	2200	2200	2200
λ	(J/kg°C°s)	2.0	2.0	2.0
β_t	(Pa^{-1})	1×10^{-9}	variable	variable
r_w	(m)	.1	.1	.1
s	(-)	0, 2, 5	0	0
T_{in}	(°C)	20	50	20
T_r	(°C)	250	250	20
k_{ri}	(-)	1	1	.714
ρ_i	(kg/m^3)	1005	996	1005
μ_i	(Pa.s)	10^{-3}	5.4×10^{-4}	10^{-3}
k_{ro}	(-)	1	1	.750
ρ_o	(kg/m^3)	800	800	800
μ_o	(Pa.s)	10^{-4}	10^{-4}	10^{-2}

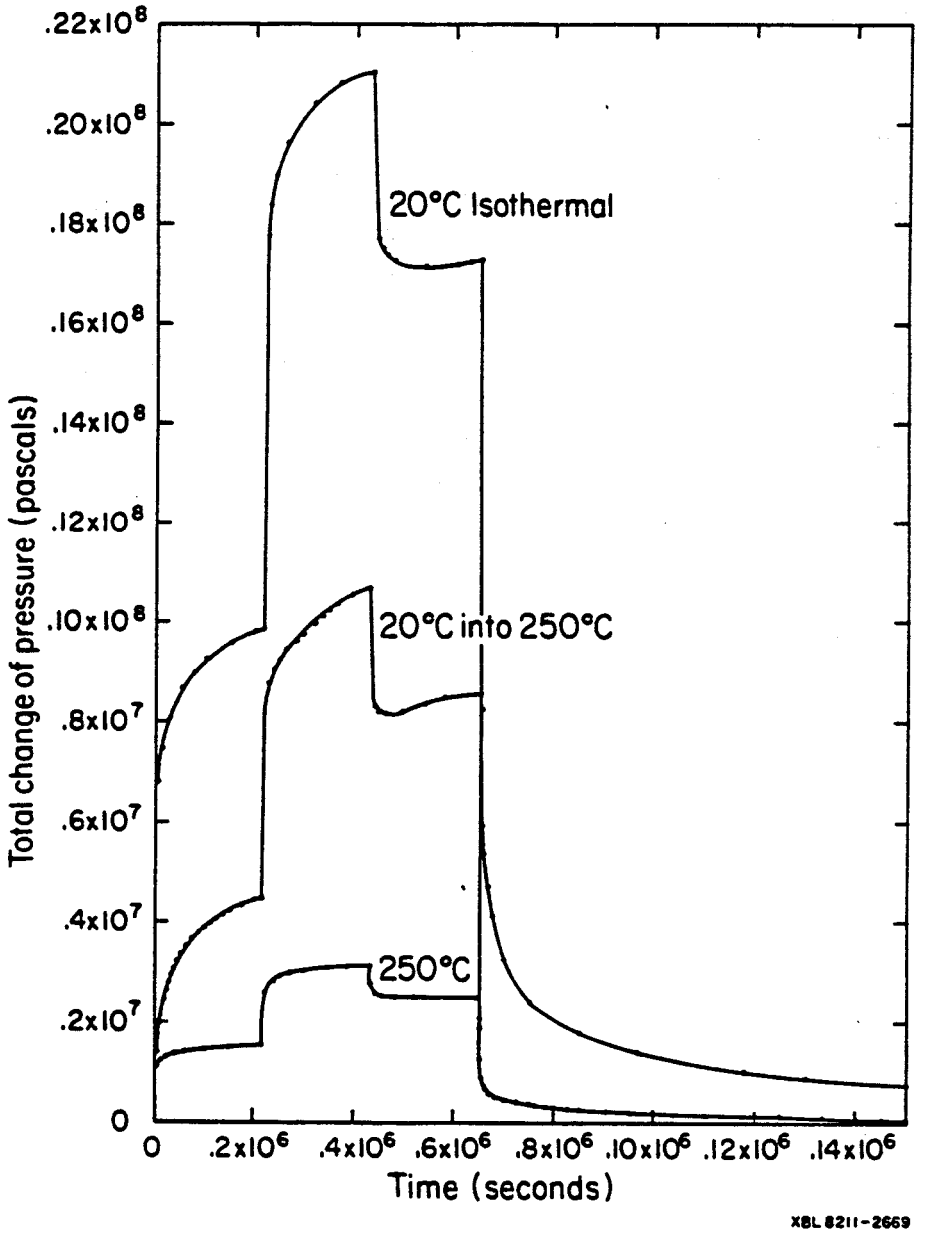

Figure 1. Simulated pressure buildup data during three steprate tests; isothermal 250°C injection, nonisothermal injection of 20°C water into a 250°C reservoir and isothermal 20°C injection.

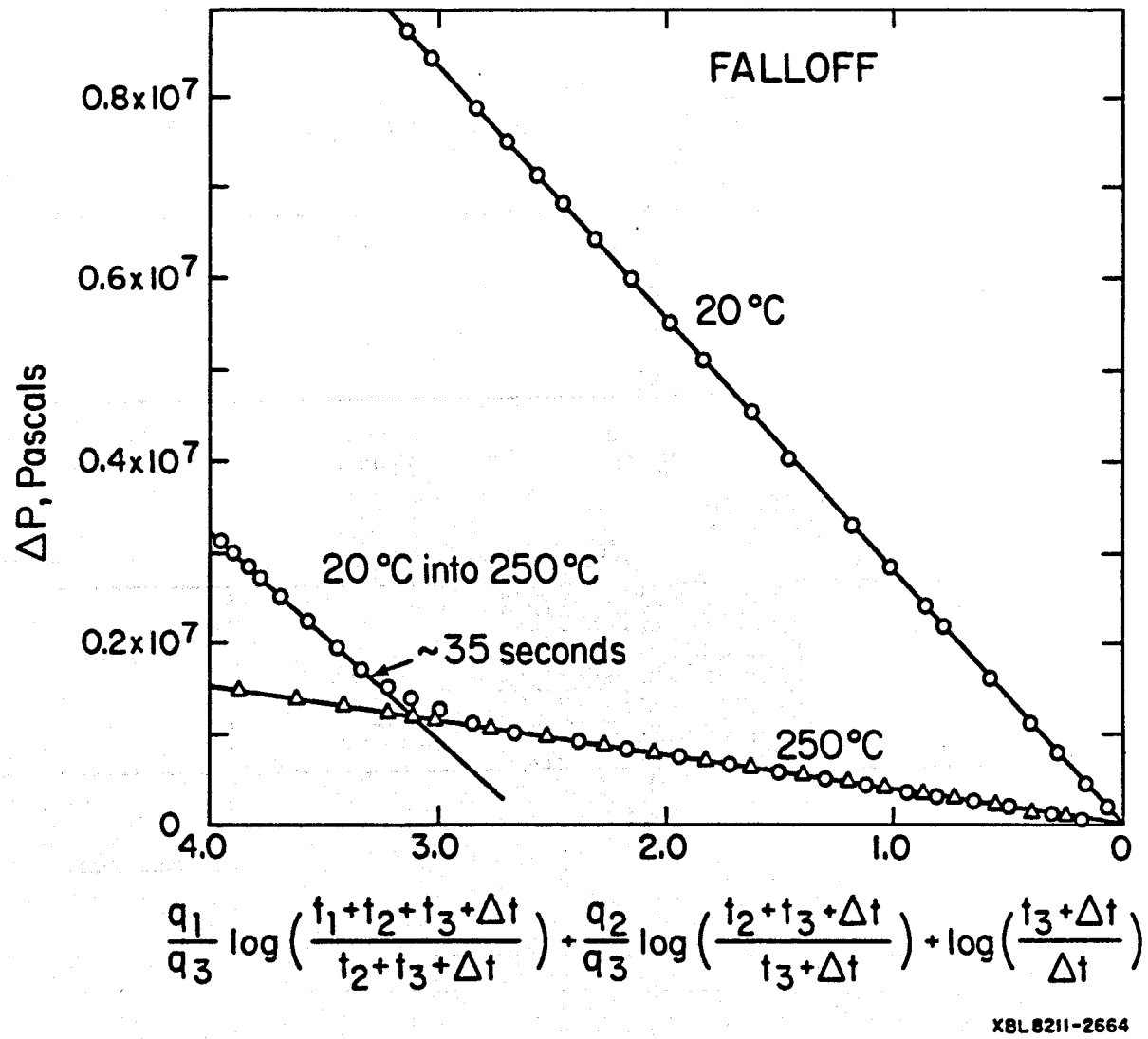

Figure 3. Pressure falloff data following the step-rate injection test shown in Figure 1.

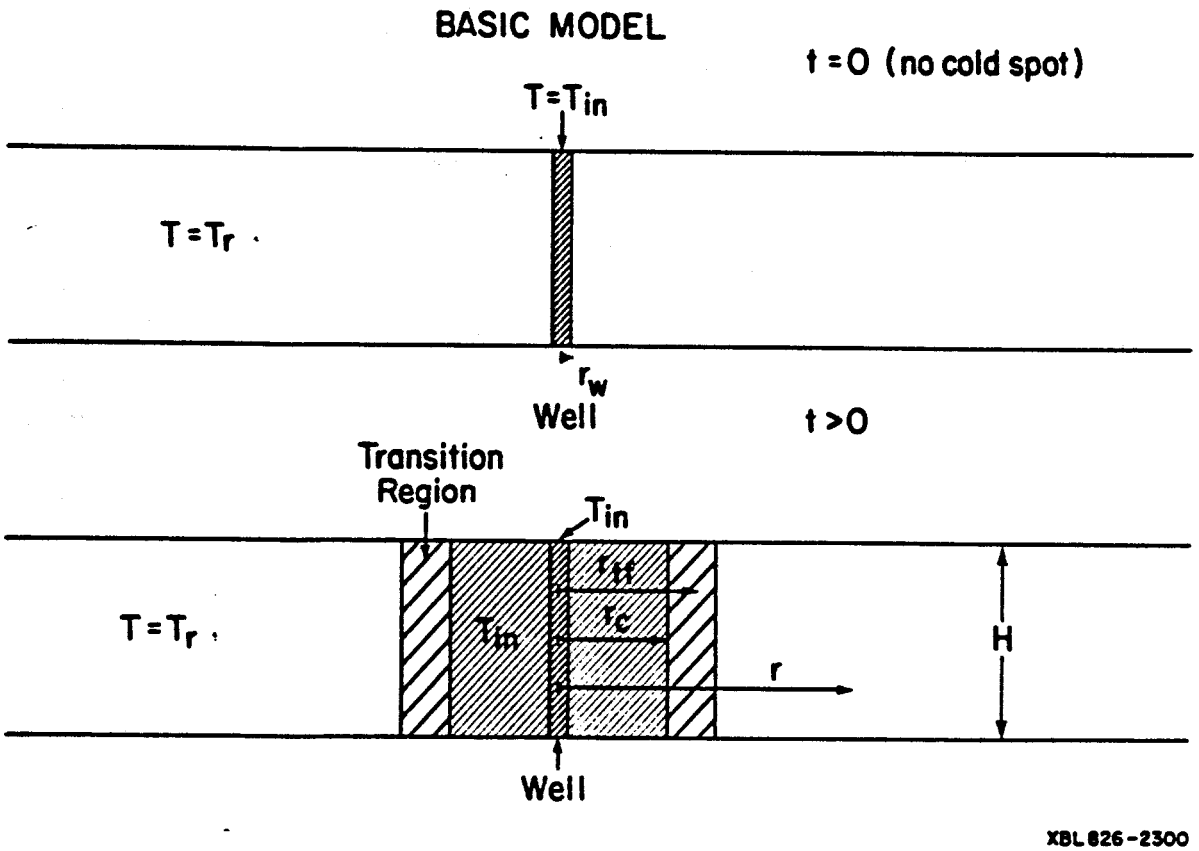

Figure 2. Schematic of well and reservoir system.

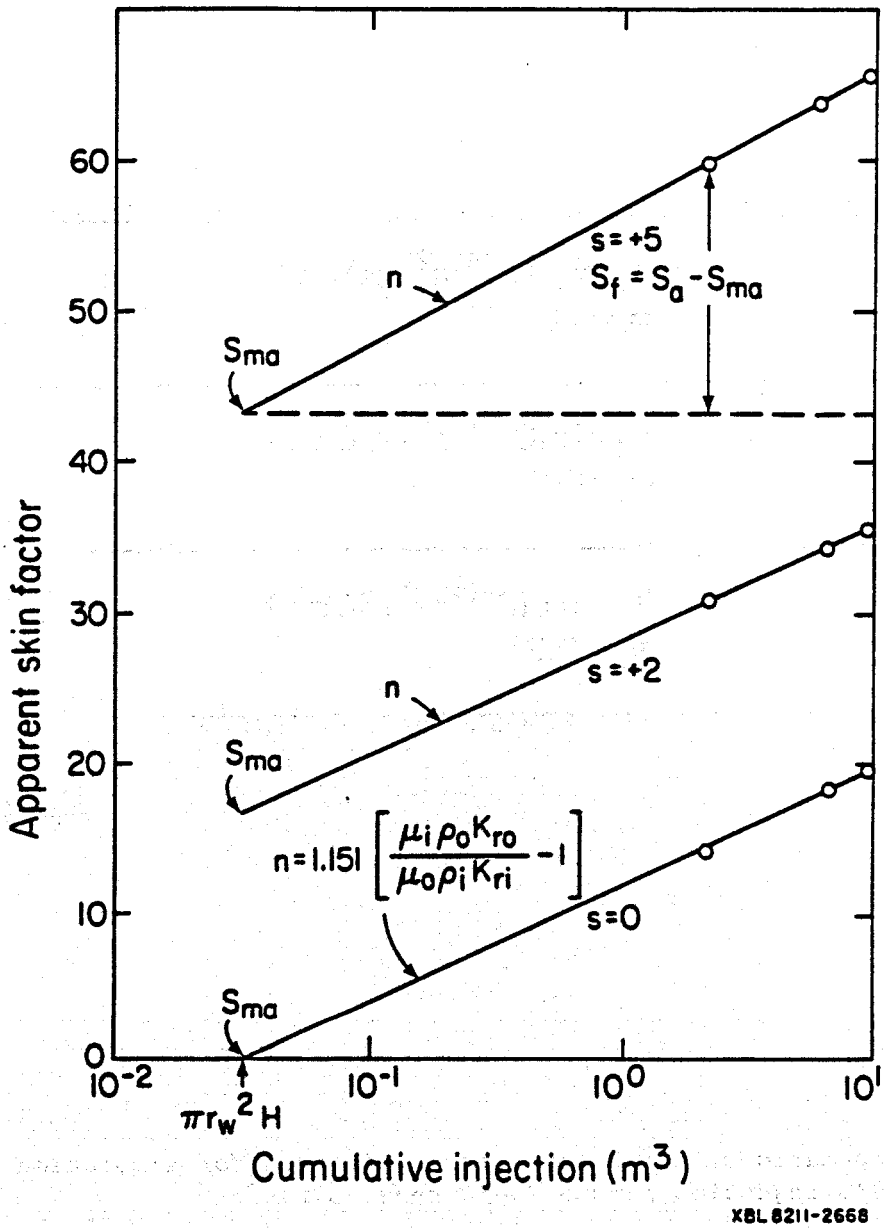

Figure 4. Calculated apparent skin factors vs. the logarithm of the cumulative injection for the step-rate test.

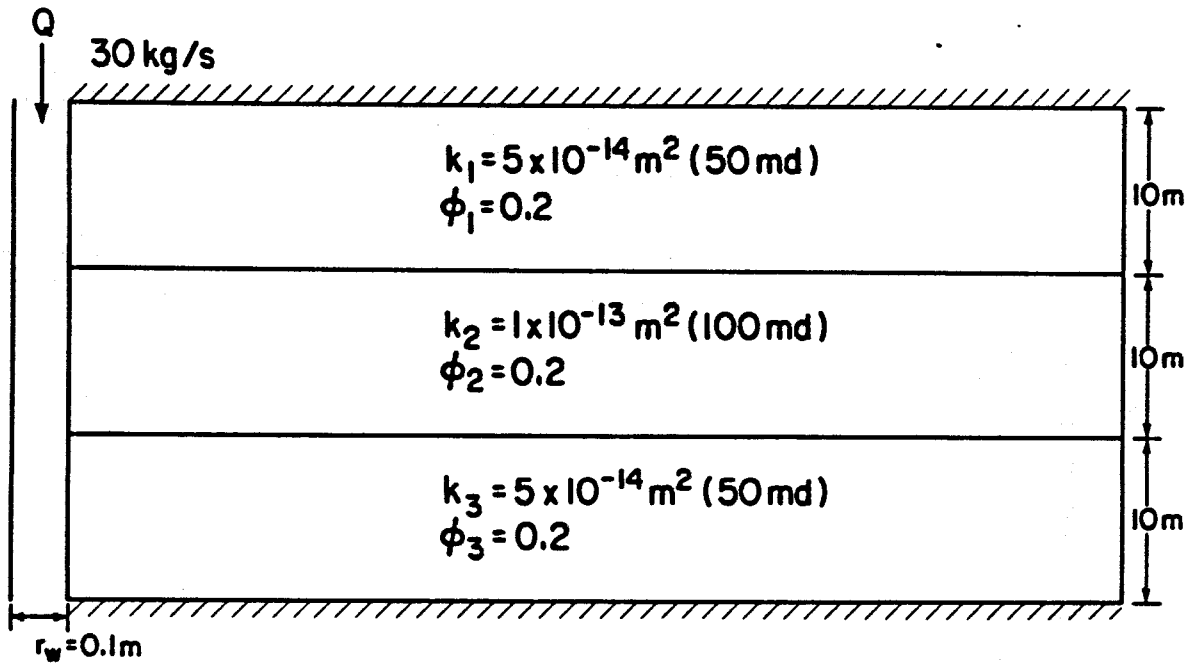

Figure 5. Schematic of the 3-layer reservoir used for simulation of 50°C injection into a 250°C reservoir.

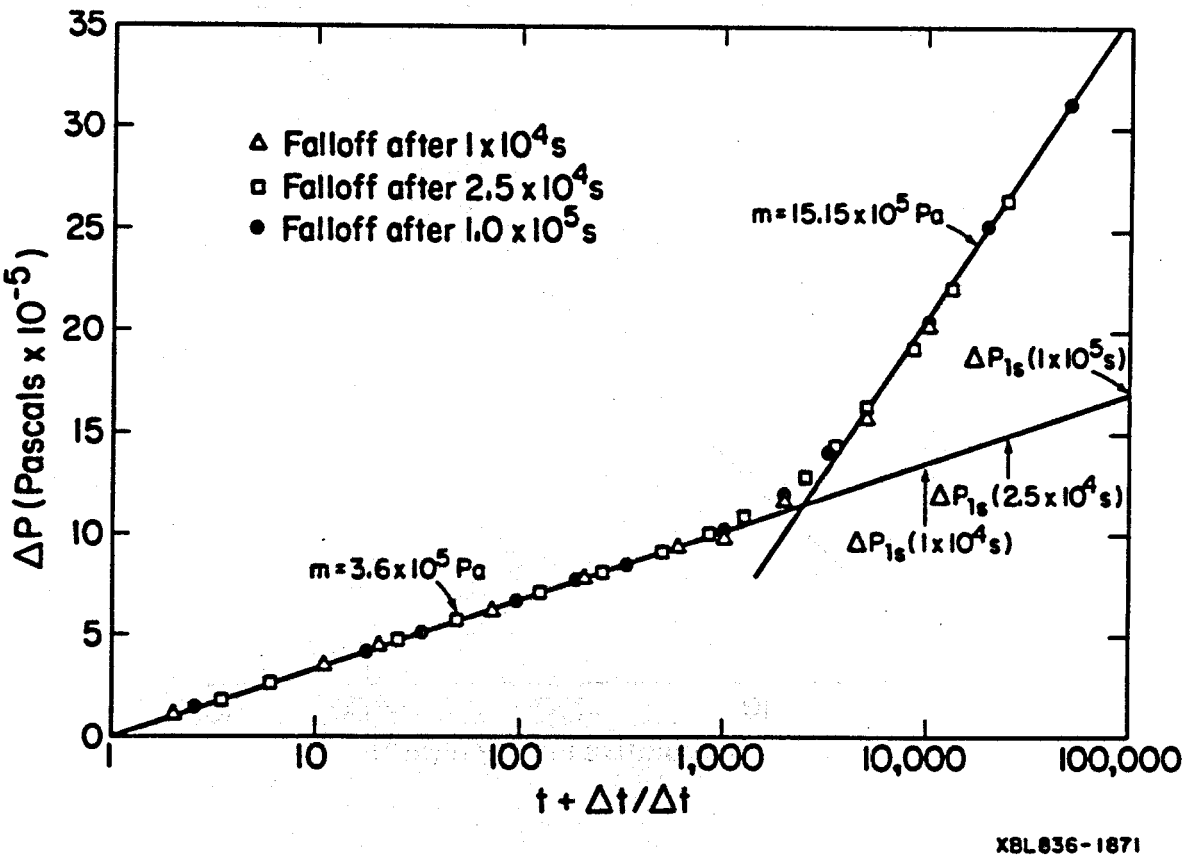

Figure 6. Horner plots of pressure buildup data, in a 3-layer reservoir, following injection of 50°C water into a 250°C reservoir.

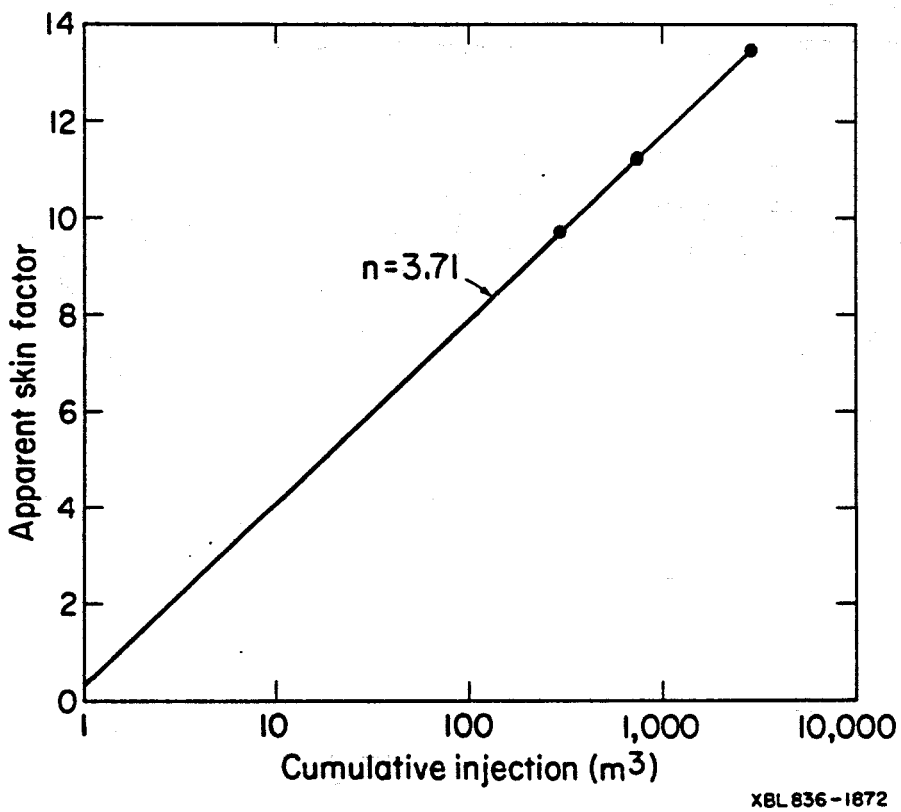

Figure 7. Apparent skin factors vs. cumulative injection for 50°C injection into a 3-layer 250°C reservoir.

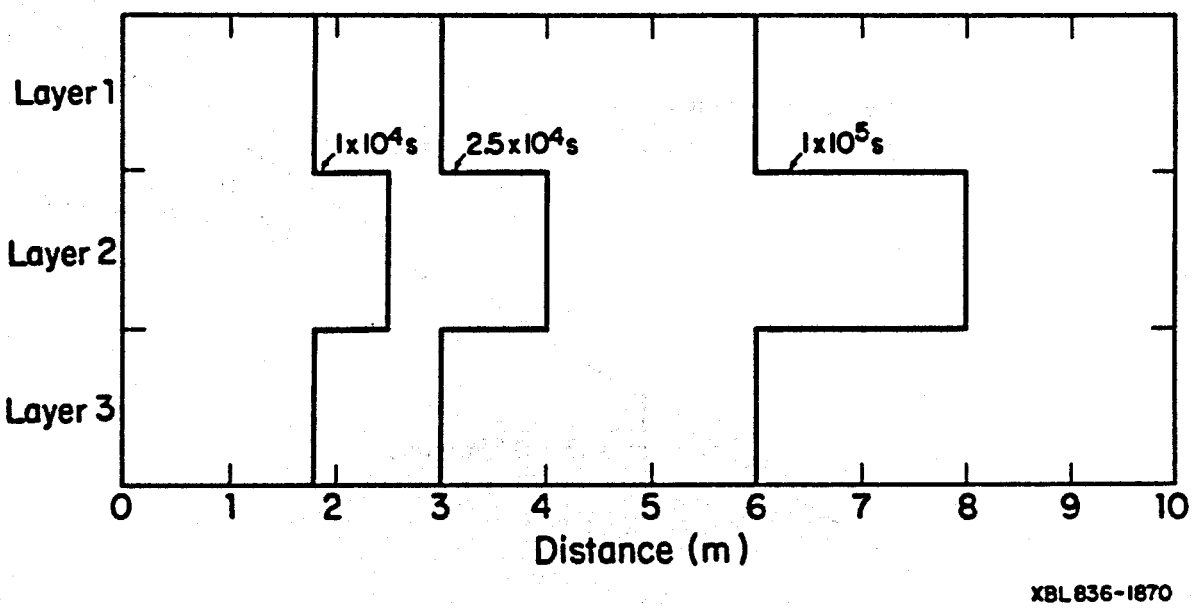

Figure 8. Radial distance to the thermal front in a three layer reservoir after 10^4s, 2.5 x 10^4s and 10^5s of injection

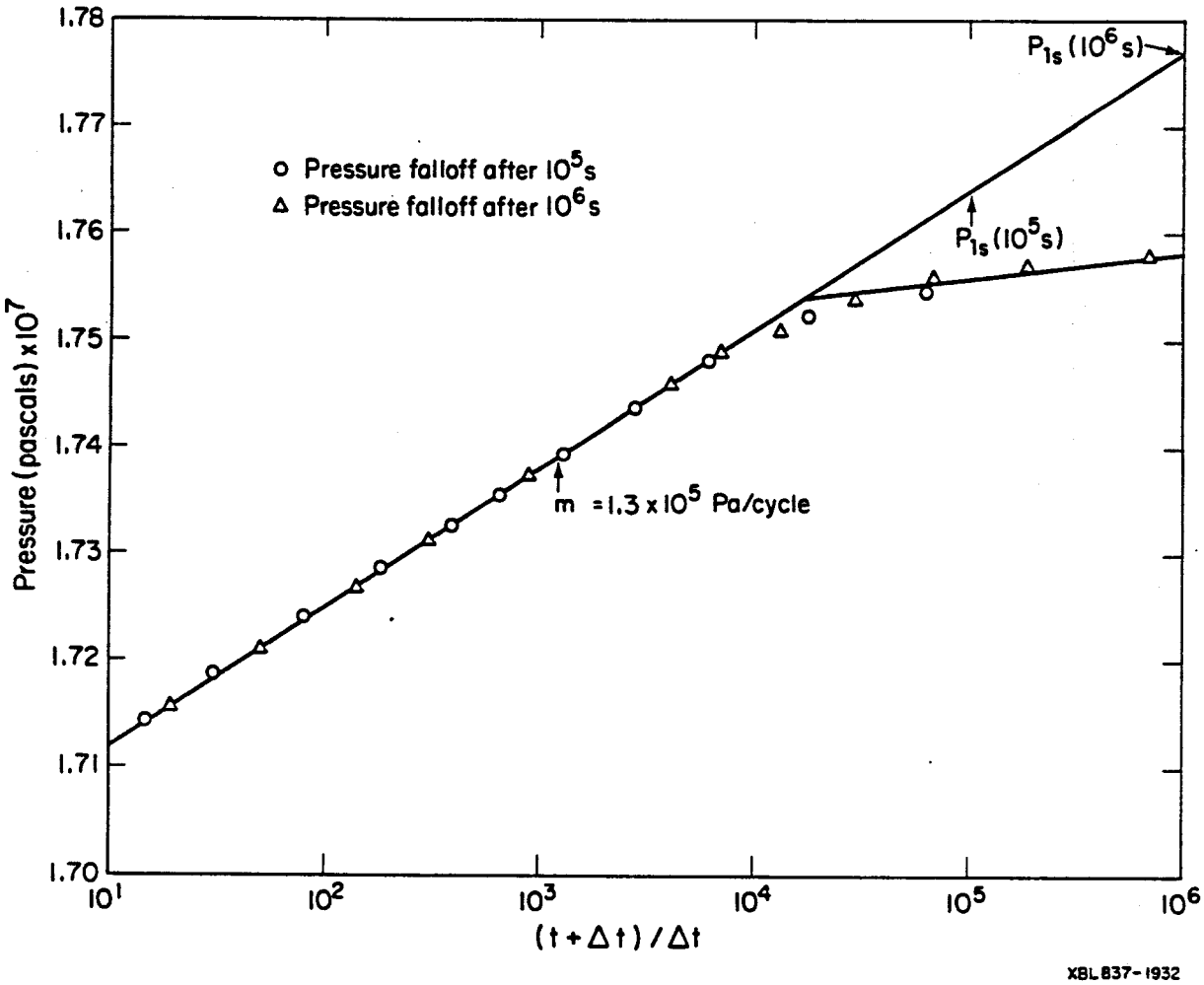

Figure 9. Horner plots of the pressure falloffs after water flooding for 10^5s and 10^6s at a rate of 05 ks/s.

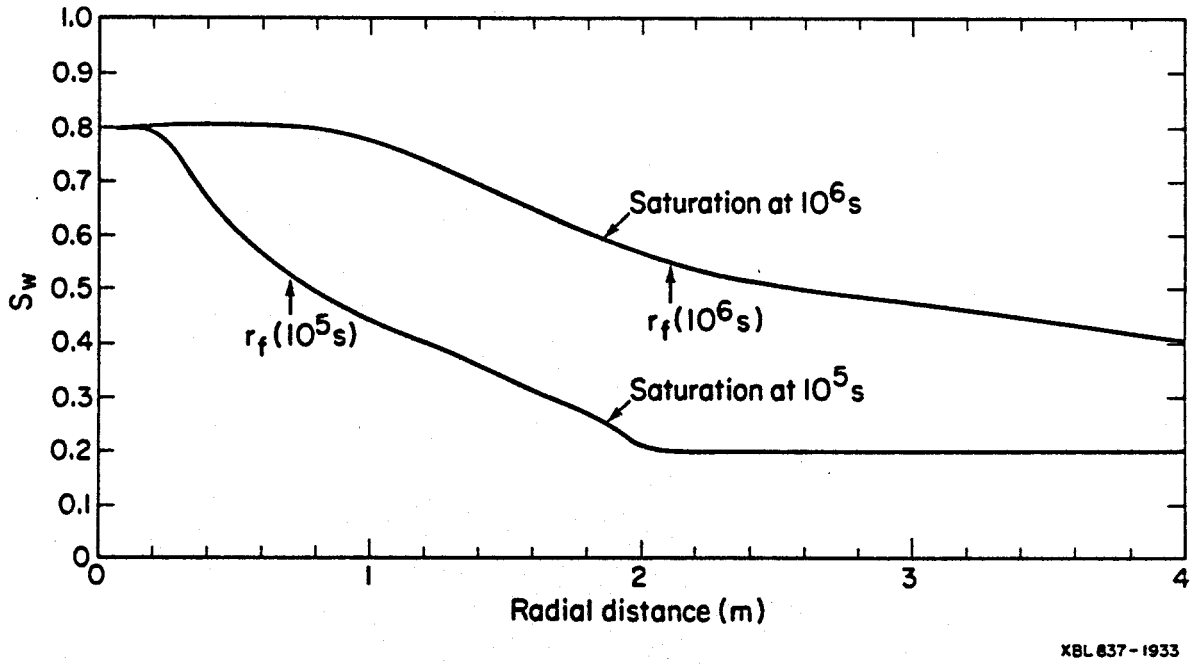

Figure 10. Saturation profiles in a water flooded oil reservoir after 10^5s and 10^6s of injection.